

Analysis of Structure and Interactions Between Chemical Reactions, Species Transport and Heat Release in Laminar Flames

Liang Ji*, Kalyanasundaram Seshadri*

University of California, San Diego, La Jolla, California 92093-0411, USA

Abstract

A novel method for analyzing counterflow diffusion flames, inspired by Zurdada's sensitivity approach for neural networks, is proposed to identify critical species influencing the heat release rate. By further analyzing concentration changes, this method reveals complex interactions among critical radicals across different temperature zones. To illustrate this approach, the study investigates the auto-ignition temperature of n-heptane and ethanol mixtures within a counterflow flame configuration under low strain rates. In n-heptane dominant mixtures, the inhibition of low-temperature chemistry (LTC) by additional ethanol impacts the heat release rate in the high-temperature zone through the diffusion of specific radicals such as CH_2O , C_2H_4 , C_3H_6 , and H_2O_2 . In ethanol-dominant mixtures, higher ethanol fractions increase the heat release rate, primarily due to ethanol decomposition and its subsequent reactions. This method effectively quantifies and compares the influence of both chemical kinetics and species diffusion effects, providing detailed insights into the interactions among species across the reactive field when analyzing the counterflow configuration of complex fuel mixtures.

Keywords: nonpremixed flows; autoignition; Low temperature chemistry; n-heptane; ethanol; sensitivity analysis

*Corresponding authors: kseshadri@ucsd.edu, lji@ucsd.edu

1. Introduction

The laminar counterflow diffusion flame, as a steady state and one dimensional flame, is investigated to elucidate interaction between diffusion and chemistry[1]. This configuration has been widely studied to improve understanding of mechanism of inhibition effect and dilution limits[2][3][4].

Through the counterflow configuration, Seshadri [2] studied extinction of diffusion flame methanol, heptane and wood in the presence of suppressive agents such as nitrogen and water. Seiser et al. [3] elucidated the mechanisms of extinction and autoignition of n-heptane, finding that strain has greater influence on low-temperature chemistry than the temperature of the reactants. Ji et al. [4] investigated the impact of iso-butanol and ethanol on the auto-ignition of n-decane and n-heptane. It is observed that addition of iso-butanol and ethanol to n-decane or n-heptane elevated the auto-ignition temperature at low strain rates, indicating that iso-butanol and ethanol inhibits the low-temperature chemistry (LTC) of n-decane and n-heptane. These observations were further supported by sensitivity analysis.

Sensitivity analysis have been extensively employed to elucidate the influence of selected parameters on combustion. They are useful for identification and quantification of the role of selected parameters, reveal their predominant controlling influence alongside their indirect effect on changes in their values [5]. It is crucial in uncertainty analysis, estimation of parameter, and investigation or reduction of mechanism [6]. This approach is instrumental in understanding the sensitivity of the predicted outcomes or quantities of interest (QoIs) to uncertain parameters [7]. For example, sensitivity analysis facilitates quantification of the indirect influence of the rate constants of reactions in terms of temperature. However, the traditional sensitivity analysis in combustion research focuses on the systematic impact of parameters on output variables. It falls short of detailed explaining the direct influence between reactions and the output variables, nor the subsequent effects of these output variables changes on other output variables.

Another widely used method, path flux analysis (PFA) method, plays a crucial role in dissecting the production and consumption fluxes (pathways) in chemical mechanism. It is employed alongside in direct relation graph (DRG) method to identify critical species and reactions. Sun et al. demonstrated that the skeletal mechanisms refined by PFA exhibits enhanced accuracy compared to those derived by DRG method with the similar size in several cases[8] [9]. Path flux analysis could explicitly offer insight into the consumption and production of species in zero-dimensional models or single point in one-dimensional flame configura-

tion, facilitating analysis of kinetic mechanism. However, for the counterflow flame configuration, it has difficulty in elucidating the interaction cross different spatial points.

Recently, there have been numerous studies applying deep learning to chemical ordinary differential equations (ODEs). Ji et al.[10] developed the stiff-PINN approach that utilizes QSSA to enable the PINN to solve stiff chemical kinetics. The multiscale physics-informed neural network (MPINN) approach proposed by Weng et al.[11] is based on the regular physics-informed neural network (PINN) for solving stiff chemical kinetic problems with governing equations of stiff ODEs. Su et al.[12] employed a neural ordinary differential equation (Neural ODE) framework to optimize the kinetic parameters of reaction mechanisms, showing that the proposed algorithm can optimize stiff chemical models with sufficient accuracy, efficiency, and robustness. The forward propagation in neural networks shows a kind of equivalence to chemical ODEs. Thus, it is also possible to introduce sensitivity analysis methods for neural networks to chemical systems.

Zurada's sensitivity method, widely used in the analysis of neural networks for the reduction of training set size[13], employs the calculation of partial derivatives with respect to variables to elucidate their interdependencies. Inspired by Zurada's method and considering the unique characteristics of combustion chemistry alongside the governing equations of the counterflow configuration, we introduce a supplemental method. This method, grounded in the use of partial derivatives, aims to analyze the interplay across different temperature zones in counterflow flames. It is employed to provide a detailed explanation of the interactions between n-heptane and ethanol in their binary mixtures in counterflow diffusion flames.

2. Methodology

2.1. Analysis of reaction rate change

The objective of the analysis is to identify factors, either changes in value of the rate constant, species concentration or both, that primarily contribute to variations of the reaction rate under selected conditions.

The rates of forward reaction $\dot{\omega}_{f,k}$ and reverse reaction $\dot{\omega}_{b,k}$ of the k^{th} reversible reaction are determined by the product of the concentration of species i , c_i and their respective rate constants $k_{f,k}$ and $k_{b,k}$. Hence, $\dot{\omega}_{f,k} = k_{f,k} \prod_{i=1}^m c_i^{\nu'_i}$, $\dot{\omega}_{b,k} = k_{b,k} \prod_{i=1}^m c_i^{\nu''_i}$, where the parameters ν'_i , ν''_i represent the stoichiometric coefficients

for species i appearing as a reactant and as a product in a reversible reaction, respectively.

In the analysis described here, forward and reverse steps of an elementary reaction is considered to be two separate reactions. Thus if there are M reversible reactions, the total number of reactions considered as $2M$.

$$\dot{\omega}_n = \begin{cases} \dot{\omega}_{f,k}, n = 2k - 1, \text{(for forward reaction)} \\ \dot{\omega}_{b,k}, n = 2k, \text{(for reverse reaction)} \end{cases} \quad \text{where } k = 1, 2, \dots, M \quad (1)$$

Here, i denotes the i^{th} reversible elementary reactions before their separation into forward and reverse components, while n represents the n^{th} reactions after separation. The total number of reactions after separation is N .

Similar to the approach taken in sensitivity analysis, the calculation of partial derivatives of the n^{th} reaction rate, $\dot{\omega}_n$, with respect to the rate constant, k_n , and species concentration, c_i , is a key parameter in reaction-rate-change-analysis.

Let $\Delta\dot{\omega}_n$ represent the difference in the value of $\dot{\omega}_n$ as a result of changes in the input variables, for example changes in initial composition of the reactive mixture. Let the corresponding changes in value of the rate constant k_n and concentration of species i be Δk_n and Δc_i , respectively. It follows that,

$$\begin{aligned} \Delta\dot{\omega}_n|_{k_n} &= \Delta\dot{\omega}_n \times \frac{\partial\dot{\omega}_n/\partial k_n \times \Delta k_n}{\Delta\dot{\omega}_n^{\text{approx}}} \\ \Delta\dot{\omega}_n|_{c_i} &= \Delta\dot{\omega}_n \times \frac{\partial\dot{\omega}_n/\partial c_i \times \Delta c_i}{\Delta\dot{\omega}_n^{\text{approx}}} \end{aligned} \quad (2)$$

where $\Delta\dot{\omega}_n|_{k_n}$ and $\Delta\dot{\omega}_n|_{c_i}$ are change of reaction rate caused by Δk_n and Δc_i . And the derivatives $\Delta\dot{\omega}_n^{\text{approx}}$, $\partial\dot{\omega}_n/\partial k_n$ and $\partial\dot{\omega}_n/\partial c_i$ are given by:

$$\begin{aligned} \Delta\dot{\omega}_n^{\text{approx}} &= \frac{\partial\dot{\omega}_n}{\partial k_n} \times \Delta k_n + \sum_{i=1}^m \left(\frac{\partial\dot{\omega}_n}{\partial c_i} \times \Delta c_i \right) \\ \frac{\partial\dot{\omega}_n}{\partial k_n} &= \prod_{i=1}^m c_i^{|\nu_i|}, \frac{\partial\dot{\omega}_n}{\partial c_i} = k_n \nu_i c_i^{|\nu_i|-1} \prod_{\substack{j=1 \\ i \neq j}}^m c_j^{|\nu_j|} \end{aligned} \quad (3)$$

with $\nu_i = \nu_i'' - \nu_i'$. Here, m represents the total number of species involved in the n^{th} reaction. The term $\Delta\dot{\omega}_n^{\text{approx}}$ is an approximation of $\Delta\dot{\omega}_n$, derived from the Taylor expansion truncated at the first-order derivative. A second-order Taylor series expansion can be employed if improved accuracy is desired especially in evaluation of $\dot{\omega}_n$. Details are provided in Appendix B.1.

2.2. Analysis of heat release rate change

The goal of the heat-release-rate-analysis is to provide quantitative information concerning the impact of changes in concentration each species on overall heat release rate, \dot{Q} , under different input boundary conditions. The quantity $\dot{Q} = \sum_k \Delta H_k \times \dot{\omega}_k$, where ΔH_k and $\dot{\omega}_k$ are, respectively, the enthalpy change and net reaction rate of the k^{th} reaction. Furthermore, the net reaction rate $\dot{\omega}_k = \dot{\omega}_{f,k} - \dot{\omega}_{b,k}$. Hence, through separation operation, Eqn. (1), it follows that

$$\dot{Q} = - \sum_n \Delta H_n \times \dot{\omega}_n \quad (4)$$

Heat-release-rate-analysis presented here is primarily focused on region where the temperature is the highest with the input enthalpy of the reactant streams maintained at constant values. Therefore, the local temperature at selected points for different input values are nearly the same allowing for the reasonable assumption that reaction enthalpy ΔH_n , which depends on local temperature, remains constant. Therefore, the contribution to change of heat release rate, $\Delta \dot{Q}$, arising from changes in rate constant, Δk_n and species concentrations Δc_i , are written as follows:

$$\Delta \dot{Q}|_{k,n} = -\Delta H_n \times \Delta \dot{\omega}_n|_{k,n} \quad (5)$$

$$\Delta \dot{Q}|_{c_i} = \sum_n (-\Delta H_n \times \Delta \dot{\omega}_n|_{c_i}) \quad (6)$$

The terms $\Delta \dot{Q}|_{k,n}$, and $\Delta \dot{Q}|_{c_i}$ represent the change of heat release rate attributed to the change in value of rate constant Δk_n and the change in value of concentration of species i , Δc_i of the n^{th} reaction.

2.3. Analysis of species concentration change

The goal of the analysis of species concentration change is to provide quantitative information concerning the impact of changes in rates of reactions on changes in concentration of species and elucidate the interaction among various species, particularly for those for which steady-state approximation are reasonably accurate. For species that do not satisfy steady-state approximation, the analysis includes the effects of species diffusion and convection on concentration. Furthermore, diagrams illustrating species equation terms provides a visual representation that enhances understanding interactions associated with these species.

As an example for the counterflow flame the steady state balance equation for species i is given by :

$$0 = -\rho u \frac{dY_i}{dz} - \frac{dj_i}{dz} + W_i(\dot{\omega}_i^+ - \dot{\omega}_i^-) \quad (7)$$

Here, z represents the spatial co-ordinate, ρ the density, u the mass-averaged velocity, Y_i , and W_i are the mass fraction and molecular weight of species i , j_i the diffusive flux of species i , and $\dot{\omega}_i^+$ and $\dot{\omega}_i^-$ are, respectively the rate of production and rate of consumption of species i . The first term on the right side of Eqn. (7) represents convective transport, the second term diffusive transport, and the third term the net rate of production of species i . From Eqn. (7) and expression obtained for c_i is obtained and written as

$$c_i = \frac{-\rho u \frac{dY_i}{dz} / W_i - \frac{dj_i}{dz} / W_i + \sum_k |\nu_{i,k}| [(1 - \delta'_{i,k})\dot{\omega}_{f,k} + \delta'_{i,k}\dot{\omega}_{b,k}]}{\sum_k |\nu_{i,k}| [\delta'_{i,k}w_{f,k}^{den} + (1 - \delta'_{i,k})w_{b,k}^{den}]} \quad (8)$$

Here, $\delta'_{i,k}$ defined as

$$\delta'_{i,k} = \begin{cases} 1 & \text{if } \nu_{i,k} < 0, \\ 0 & \text{if } \nu_{i,k} > 0 \end{cases} \quad (9)$$

The term $\nu_{i,k}$ is given by $\nu''_{i,k} - \nu'_{i,k}$, where $\nu'_{i,k}$, $\nu''_{i,k}$ are the stoichiometric coefficients for species i appearing as a reactant and as a product in k^{th} reaction, respectively. The detailed derivation of Eqn. (8) is shown in Appendix B.2. In Eqn. (8), the terms $[-\rho u \frac{dY_i}{dz} / W_i]$ and $[-\frac{dj_i}{dz} / W_i]$ correspond to convective and diffusive mass transfer related term of species i , respectively. These terms can be neglected if steady-state approximation is satisfied. The term $\sum_k |\nu_{i,k}| [(1 - \delta'_{i,k})\dot{\omega}_{f,k} + \delta'_{i,k}\dot{\omega}_{b,k}]$ accounts for all reactions producing species i while $\sum_k |\nu_{i,k}| [\delta'_{i,k}w_{f,k}^{den} + (1 - \delta'_{i,k})w_{b,k}^{den}]$ accounts for all reactions consumed species i .

The framework described by Eqn. (8), is used to analyze changes in the concentration of species i . For the k^{th} elemental reaction, the contribution of its forward reaction rate with respect to species c_i is:

$$\Delta c_i|_{f,k} = \begin{cases} \frac{1}{\text{sum}} \times \frac{\partial c_i}{\partial w_{f,k}} \times \Delta w_{f,k}, & \nu_{i,k} > 0 \\ \frac{1}{\text{sum}} \times \frac{\partial c_i}{\partial w_{f,k}^{den}} \times \Delta w_{f,k}^{den}, & \nu_{i,k} < 0 \end{cases} \quad (10)$$

Similarly, its backward reaction rate contribution with respect to c_i is expressed as:

$$\Delta c_i|_{b,k} = \begin{cases} \frac{1}{\text{sum}} \times \frac{\partial c_i}{\partial w_{b,k}} \times \Delta w_{b,k}, \nu_{i,k} < 0 \\ \frac{1}{\text{sum}} \times \frac{\partial c_i}{\partial w_{b,k}^{\text{den}}} \times \Delta w_{b,k}^{\text{den}}, \nu_{i,k} > 0 \end{cases} \quad (11)$$

The contributions of convective mass transfer with respect to changes in c_i are identified as:

$$\Delta c_i|_{\text{convection}} = \frac{1}{\text{sum}} \times \frac{\partial c_i}{\partial (\rho u \frac{dY_i}{dz})} \times \Delta (\rho u \frac{dY_i}{dz}) \quad (12)$$

Similarly, the contributions of diffusion mass transfer with respect to changes in c_i is expressed as:

$$\Delta c_i|_{\text{diffusion}} = \frac{1}{\text{sum}} \times \frac{\partial c_i}{\partial (\frac{dj_i}{dz})} \times \Delta (\frac{dj_i}{dz}) \quad (13)$$

Here, sum defined as the aggregate of all contributions to changes in c_i , encapsulating those from both the forward and backward reaction rates, as well as from the convective and diffusive mass transfers:

$$\begin{aligned} \text{sum} = & \sum \frac{\partial c_i}{\partial w_{f,k}} \times \Delta w_{f,k} + \sum \frac{\partial c_i}{\partial w_{f,k}^{\text{den}}} \times \Delta w_{f,k}^{\text{den}} \\ & + \sum \frac{\partial c_i}{\partial w_{f,k}^{\text{den}}} \times \Delta w_{f,k} + \sum \frac{\partial c_i}{\partial w_{b,k}^{\text{den}}} \times \Delta w_{b,k}^{\text{den}} \\ & + \frac{\partial c_i}{\partial (\rho u \frac{dY_i}{dz})} \times \Delta (\rho u \frac{dY_i}{dz}) + \frac{\partial c_i}{\partial (\frac{dj_i}{dz})} \times \Delta (\frac{dj_i}{dz}) \end{aligned} \quad (14)$$

It has been established that for a species for which steady-state approximation is accurate, the magnitudes of both the rate of production and the rate of consumption are much larger than the sum of the magnitudes of the convective and diffusive terms [14]. Consequently, upon neglecting the diffusion and convection terms, the concentration of species i , as depicted in Eqn. (8), simplifies to:

$$c_i = \frac{\sum_{k=1}^r |\nu_{i,k}| [(1 - \delta'_{i,k}) w_{f,k} + \delta'_{i,k} w_{b,k}]}{\sum_{k=1}^r |\nu_{i,k}| [\delta'_{i,k} w_{f,k}^{\text{den}} + (1 - \delta'_{i,k}) w_{b,k}^{\text{den}}]} \quad (15)$$

Furthermore, the term sum simplifies in the steady-state(ss) approximation as follows:

$$\begin{aligned} \text{sum}_{ss} = & \sum \frac{\partial c_i}{\partial w_{f,k}} \times \Delta w_{f,k} + \sum \frac{\partial c_i}{\partial w_{f,k}^{den}} \times \Delta w_{f,k}^{den} \\ & + \sum \frac{\partial c_i}{\partial w_{b,k}^{den}} \times \Delta w_{b,k}^{den} + \sum \frac{\partial c_i}{\partial w_{b,k}} \times \Delta w_{b,k} \end{aligned} \quad (16)$$

In scenarios where steady-state approximation is not applicable to species c_i , it becomes critical to consider all terms in the describing equation, including those related to diffusion and convection. This comprehensive approach elucidates the relative significance of diffusion and convection and the chemical reaction term. Furthermore, for species that do not maintain steady-state, visualizing convection, diffusion and net production terms in Eqn. (7) helps to describe scenarios wherein species are produced in one region of the reaction zone transported to a different region of the reaction zone where they react. This is one of the key differences between reactions in flow systems (for example strained premixed and non-premixed flames) and non-flow systems (for example reactions in shock-tubes).

At a specific location, the dominance of one term over others in species equation highlights its pivotal role in shaping concentration profile. A positive value indicates an enhancement in concentration, whereas a negative value signifies a diminishing effect on concentration profile. This approach is elaborated in results and discussion section.

3. Demonstration of methodology

Low-temperature chemistry (LTC) is an intrinsic feature of combustion of hydrocarbons such as n-alkanes, alkenes and cycloalkanes, [15]. The LTC of n-heptane, for example, has been extensively investigated in various experimental setups, including the counterflow flame [3], shock tube[16], jet-stirred reactor[17], microgravity droplet flame [18]. Further studies have explored the impact of alcohol addition to n-heptane or other hydrocarbons in combustion characteristics[19]-[20]. While, traditional sensitivity method enhances the understanding of interactions within mechanisms, it falls short of detailing the influence between reactions and species across the reactive field.

Here, we demonstrate the use of the analysis method developed above to elucidate interaction between ethanol and n-heptane in counterflow flame. Computational results from a previous investigation [21] are used to illustrate the method.

This previous study reports on species distribution, flame structure and critical conditions of auto-ignition obtained employing the liquid-fuel counterflow configuration. These computations are performed using Cantera [22] C++ interface with modified boundary conditions at the liquid-gas interface. The mix-average transport model is applied to obtained steady-state solutions. Kinetic modeling is carried out using the San Diego Mechanism [23].

The fuels tested include n-heptane, ethanol, and their mixtures with volumetric composition of 20% n-heptane + 80% ethanol, 30% n-heptane + 70% ethanol, 50% n-heptane + 50% ethanol, 80% n-heptane + 20% ethanol, and 90% n-heptane + 10% ethanol. The oxidizer is air.

3.1. Auto-ignition temperature and heat release rate analysis

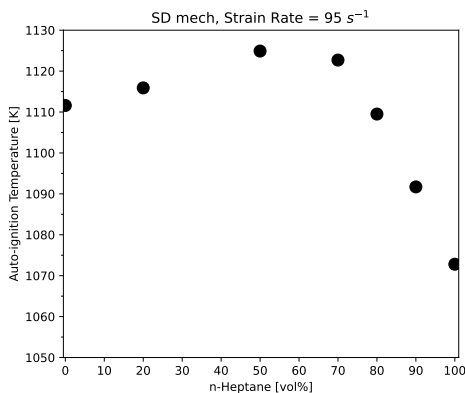


Figure 1: Auto-ignition temperature at strain rate of 95 s^{-1} .

Fig. 1 shows auto-ignition temperature calculated at low strain rate, 95 s^{-1} for various volume fractions of ethanol in n-heptane, and Fig. 2 shows the variations in heat release rate, prior to auto-ignition, for these mixtures within the high-temperature zone, particularly focusing at 4.3 mm above the liquid-gas interface and at an oxidizer temperature, T_{ox} , of 1060K. A comparison between Fig. 1 and Fig. 2 indicates a direct correlation between the magnitude of heat release rate in this zone and the requisite temperature of auto-ignition (T_{ig}). It is noteworthy that among the examined mixtures, the 50%n-heptane-50%ethanol blend stands out, because it has the highest value of ignition temperature, T_{ig} , a phenomenon that can be attributed to its lowest peak in heat release rate.

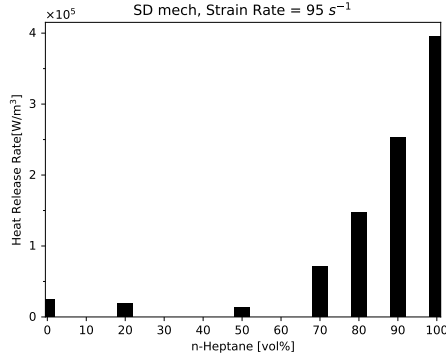


Figure 2: Heat release rate in the high-temperature zone [$T_{\text{ox}}=1060$ K]

Fig. 2 shows that the reduction of the volume fraction of heptane from 100% to 90% leads to a significant decrease in heat release rate. Furthermore heat-release-rate-analysis, as depicted in Fig. 3, directly attributes this decline of heat release rate predominantly to changes of concentrations of HCO, HO₂, OH, C₂H₅, C₂H₃, CH₂O. In contrast, the reduction in volume fraction of n-heptane from 50% to 20% correlates to an observable increase in heat release rate, as shown in Fig. 2. Similar results of heat-release-rate-analysis shown in Fig. 4 attributes the increase of heat release rate to involvement of species such as CH₃, HO₂, OH, HCO, C₂H₅OH, CH₃CHOH, CH₂O.

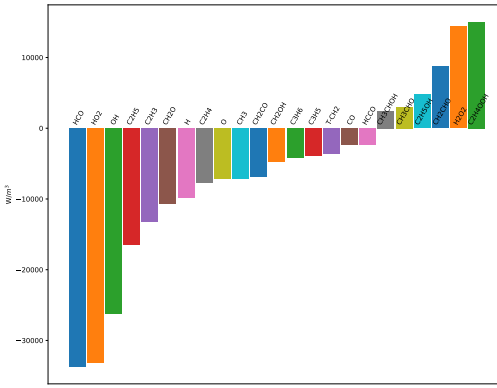


Figure 3: Distribution of heat release rate change from 100%n-heptane to 90%n-heptane

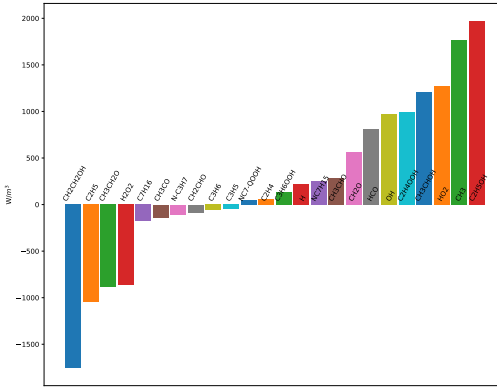


Figure 4: Heat release rate change from 50% n-heptane to 20% n-heptane

3.2. Key species in *n*-heptane-dominant mixtures

The species contributing to heat release rate change could be placed in two groups; one that can be considered to maintain steady-state at a selected location, and the other that does not maintain steady-state.

For species that do not satisfy steady-state approximation, their concentrations are governed by a species equation that includes diffusion term, convection term and chemical reaction term. Specifically, in Fig. 5, for CH_2O , that does not maintain steady-state the peak in the net production is observed around 1.2 mm, that is located in a zone where the LTC is highly active. Additionally, the positive values of the diffusion term between 2 mm and mm elucidate the role of the diffusion term in promoting the transport of the CH_2O from the low-temperature zone to the high-temperature zone. Consequently, a decline of activity of LTC in the low-temperature region, caused by additional ethanol, leads to a reduction of diffusion effect, subsequently impacting heat release rate and auto-ignition at the high-temperature region. This effect is also evidenced by analysis of CH_2O concentration change, depicted in Fig. 6. The observed reduction of CH_2O in the high-temperature region is primarily attributed to a decrease in the value of the diffusion term. Similar behaviors are observed with other species, specifically hydrogenperoxide (H_2O_2), ethylene (C_3H_6), and formaldehyde (C_2H_4). The corresponding analyses and plots for these species are shown in the supplemental materials, ranging from Fig. A.20 to Fig. A.23.

For species that are considered to maintain steady-state, their concentrations are predominantly governed by the equilibrium between production and consumption rates at a selected location. Among the primary species shown in Figure 3 that

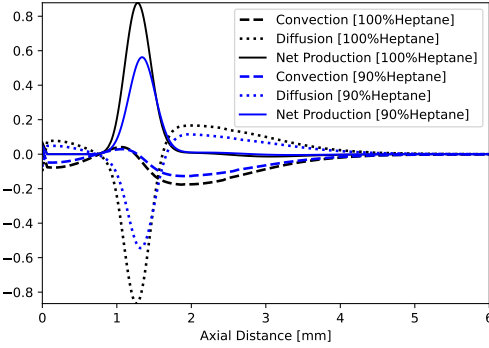


Figure 5: CH_2O Species equation terms

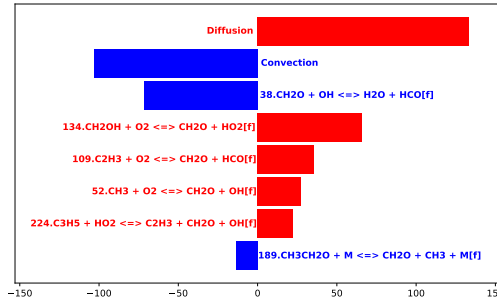


Figure 6: Contribution on CH_2O concentration change@4.2mm

leads to heat release rate reduction, HCO , HO_2 , OH , C_2H_5 and C_2H_3 are identified to be in the steady-state. This indicates these radicals are produced and consumed at approximately the same rate at the selected location. Consequently, changes in their concentrations at this location are primarily affected by certain elementary reactions, instead of species diffusion or convection. Moreover, these reactions are controlled by variations of other species in the chemical system. These related reactions and species can be further elucidated through the analysis of concentration change.

Fig. 7 demonstrates that changes in concentration of radical OH at the high-temperature zone are primarily affected by reverse reaction of R16, which is R16r: $\text{H}_2\text{O}_2 (+\text{M}) \rightarrow 2 \text{OH} (+\text{M})$, involving the decomposition of H_2O_2 ; H_2O_2 is not in steady state and is diffused from the low-temperature zone.

Further concentration analysis reveals that concentration of HO_2 is predominantly controlled by HCO , through R33f: $\text{HCO} + \text{O}_2 \rightarrow \text{CO} + \text{HO}_2$. Similarly, HCO concentration are primarily controlled by CH_2O and OH via R38f: CH_2O

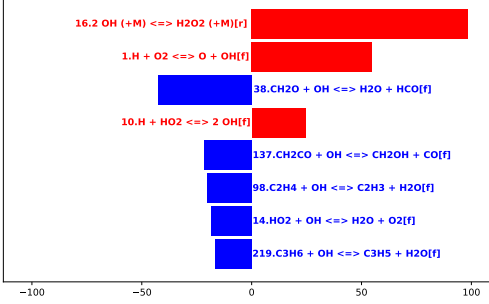


Figure 7: Contribution to OH concentration change@4.2mm

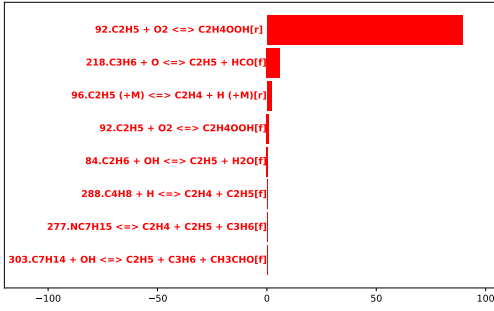


Figure 8: Contribution on C₂H₅ concentration change@4.2mm

+ OH → H₂O + HCO. Concentration of C₂H₃ is primarily regulated by C₂H₄ by R98f: C₂H₄ + OH → C₂H₃ + H₂O. Illustrative plots of these relationships are provided in the supplemental materials, as seen in Figures A.24, A.25, and A.26. As mentioned before, both CH₂O and C₂H₄ are mainly transported from the low-temperature region via diffusion.

Fig. 8 reveals that the radical C₂H₅ is primarily influenced by R92: C₂H₅+O₂ ⇌ C₂H₄OOH. However, it is actually a fast reaction so that the substantial consumption of C₂H₅ in the forward reaction is counterbalanced by its production in the reverse reaction. Therefore, greater emphasis should be placed to the second reaction depicted in Fig. 8, R218f: C₃H₆ + O → C₂H₅ + HCO, which is primarily affected by C₃H₆. Notably, C₃H₆ is not in the steady state at the high-temperature zone and is primarily diffused from the low-temperature region.

In summary, radicals including CH₂O, C₂H₄, C₃H₆ and H₂O₂ predominantly diffused from the low-temperature zone, significantly influencing the heat release rate and auto-ignition process in the high-temperature zone.

This observation underscores the necessity of delineating the production mech-

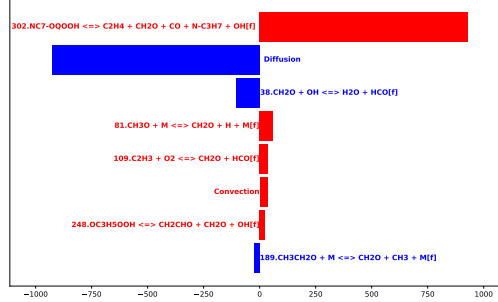


Figure 9: Contribution on CH_2O concentration change@1.1mm

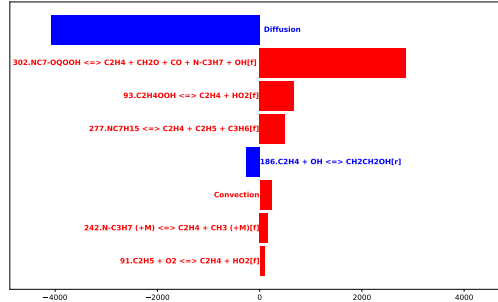


Figure 10: Contribution on C_2H_4 concentration change@1.1mm

anism of these species in the low-temperature zone. As indicated in Fig. 9 and Fig. 10, CH_2O and C_2H_4 primarily produced through reaction R302f: $\text{NC}_7\text{OQOOH} \rightarrow \text{C}_2\text{H}_4 + \text{CH}_2\text{O} + \text{CO} + \text{NC}_3\text{H}_7 + \text{OH}$ at the low-temperature zone.

The origins of C_3H_6 and H_2O_2 in the low-temperature zone is notably complex. Fig. 11 proves that concentration of C_3H_6 is predominantly regulated by NC_3H_7 . Similarly, concentration analysis of H_2O_2 and HO_2 indicate H_2O_2 is mainly converted from HO_2 , which, in turn, is affected by NC_3H_7 . These analysis results are further detailed in the supplemental materials, specifically in Figures A.27 and A.28.

Given its pivotal role, NC_3H_7 emerges as a crucial species impacting both H_2O_2 and C_3H_6 . It is primarily produced through reaction R302f, as indicated in Fig. 12. Thus, in the low-temperature region, R302f exerts a direct influence on producing CH_2O , C_2H_4 , while indirectly affecting C_3H_6 and HO_2 via NC_3H_7 .

Fig. 13 provides a comprehensive overview elucidating interplay between the low and high temperature zones in n-heptane-dominant mixtures. The addition of ethanol leads to competition of oxygen, resulting in a decreased of NC_7OQOOH

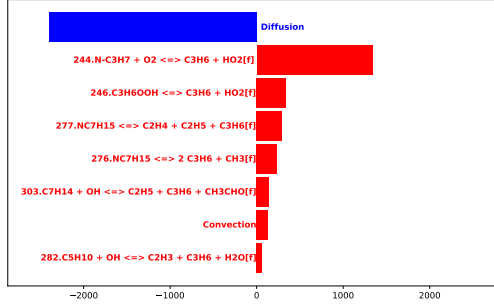


Figure 11: Contribution on C_3H_6 concentration change@1.1mm

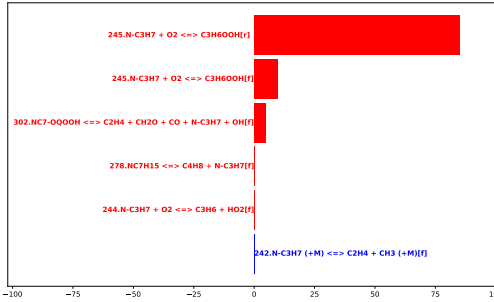


Figure 12: Contribution on NC_3H_7 concentration change@1.1mm

concentration in the low-temperature zone. This reduction in concentration of NC_7OQOOH subsequently diminishes the reaction rate of R302f and concentrations of its products. Ultimately, these effects propagated to the high-temperature zone through species diffusion.

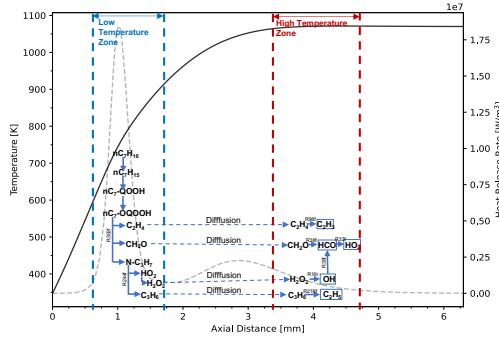


Figure 13: Heptane-dominant mixture overview. In the background, the black solid line represents the temperature profile and the grey dashed line indicates heat release rate

3.3. key species in ethanol-dominant mixtures

It is observed that a decrease of n-heptane's volume fraction from 50% to 20% and a corresponding increase in ethanol's volume fraction from 50% to 80%, results in an increase in heat release rate in the high-temperature zone. This is primarily due to the formation of three products: CH_3CHOH , $\text{CH}_2\text{CH}_2\text{OH}$ and $\text{CH}_3\text{CH}_2\text{O}$, as shown in Fig 19. These products are formed from ethanol undergoing decomposition through hydrogen abstraction. [24]

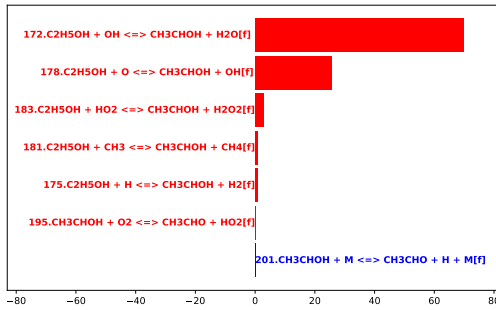


Figure 14: Contribution on CH_3CHOH concentration change@4.2mm

The production of CH_3CHOH , mainly from reactions R172f: $\text{C}_2\text{H}_5\text{OH} + \text{OH} \rightarrow \text{CH}_3\text{CHOH} + \text{H}_2\text{O}$ and R178f: $\text{C}_2\text{H}_5\text{OH} + \text{O} \rightarrow \text{CH}_3\text{CHOH} + \text{OH}$, plays a significant role in increasing heat release rate, as confirmed in Fig. 14. Notably, one pathway to form CH_3CHOH , via R183f: $\text{C}_2\text{H}_5\text{OH} + \text{H}_2\text{O}_2 \rightarrow \text{CH}_3\text{CHOH} + \text{H}_2\text{O}_2$, is accompanied by a significant production of H_2O_2 , as depicted in Fig. 15b, with the peak production around 2.0mm-2.2mm, shown in Fig. 15a. It is subsequently diffused to the high-temperature region, contributing to the increase of OH concentration through R16r, $\text{H}_2\text{O}_2 (+\text{M}) \rightarrow 2 \text{ OH} (+\text{M})$, corroborated by Fig. 16. Additionally, the reverse reaction of R186, involving the decomposition of $\text{CH}_2\text{CH}_2\text{OH}$, contributes to the elevation of OH concentration, as indicated in Fig. 16.

Furthermore, Fig. 17a demonstrates that the elevated levels of CH_3CHOH (through R195f) and $\text{CH}_3\text{CH}_2\text{O}$ (through R188f) lead to an increase in CH_3CHO . Furthermore, Fig. 17b confirms that some of the increase of CH_3CHO is by diffusion from its production peak region to the high-temperature region, thereby promoting heat release rate.

As shown in Fig. 18, the products CH_3 and CH_2O from decomposition of $\text{CH}_3\text{CH}_2\text{O}$ through R189f and from the step $\text{CH}_3\text{CH}_2\text{O} + \text{M} \rightarrow \text{CH}_2\text{O} + \text{CH}_3 + \text{M}$, diffuse to the high-temperature region. This process is augmented by R52f: CH_3

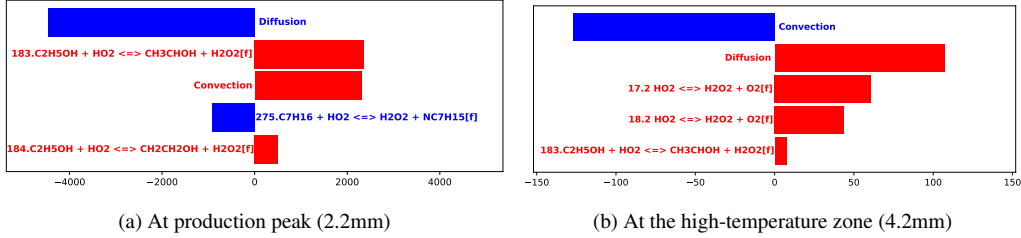


Figure 15: Contribution on H_2O_2 concentration change

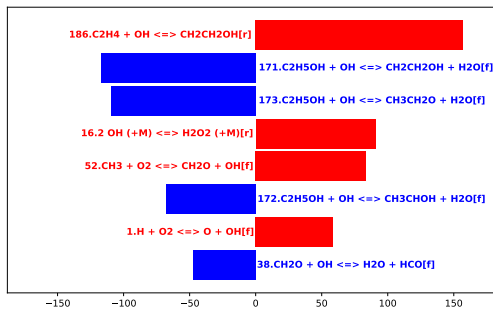


Figure 16: Contribution on OH concentration change @4.2mm

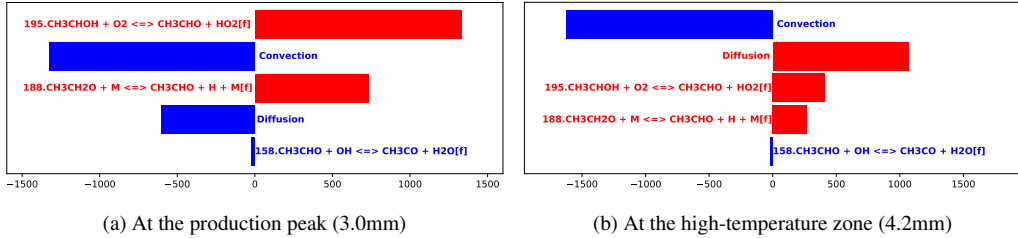


Figure 17: Contribution on CH_3CHO concentration change

$+ \text{O}_2 \rightarrow \text{CH}_2\text{O} + \text{OH}$, as illustrated in Fig A.29, wherein CH_3 reacts with O_2 , further elevating the concentration of CH_2O . The increase in CH_2O and OH leads to a rise in HCO and as a consequence to an enhanced concentration of HO_2 in the high-temperature region. The concentration change analysis related to CH_2O , HCO and HO_2 are provided in Fig. A.29, Fig. A.30 and Fig. A.31 in supplemental materials.

The reaction pathway including CH_2O , HCO and HO_2 exhibits similarity in both n-heptane-dominant and ethanol-dominant mixtures. However, the concentration of CH_2O in n-heptane-dominant mixtures is predominantly influenced by

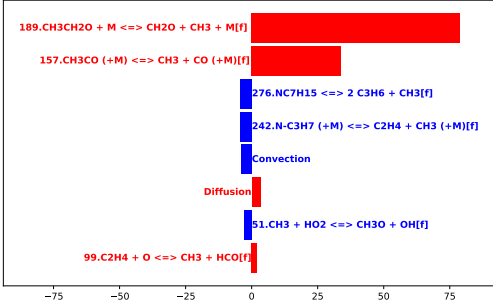


Figure 18: Contribution on CH_3 concentration change@4.2mm

the low-temperature chemistry of n-heptane, whereas in ethanol-dominant mixtures, CH_2O is significantly affected, directly and indirectly, by $\text{CH}_3\text{CH}_2\text{O}$, through ethanol's hydrogen abstraction reaction, R189.

Additionally, the increase in HO_2 partially results in heightened level of H_2O_2 at the high-temperature region, as evidenced in Fig. 15b.

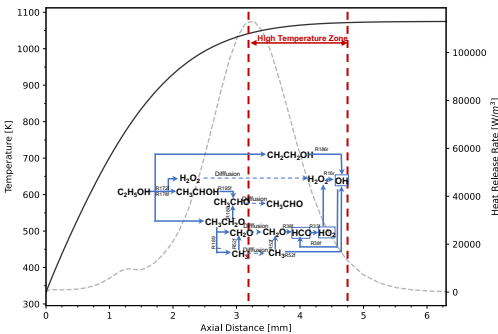


Figure 19: Ethanol-dominant mixture overview. In the background, the black solid line represents the temperature profile and the grey dashed line indicates heat release rate

Fig. 19 succinctly summarizes the reaction pathways and diffusive effects associated with ethanol-dominant mixtures. The observed increase in heat release rate, as ethanol volume fraction increased from 50% to 80%, is primarily attributable to species and reactions associated with ethanol's chemistry. In these mixtures, the influence of the inhibition of LTC is considered to be negligible.

3.4. Summary

The demonstrated example specifically concerns combustion of n-heptane and ethanol mixtures in a counterflow flame at low strain rate. Simulation results indi-

cate a correlation between heat release rate and auto-ignition temperature. Further quantitative analyses, utilizing the proposed method, reveal that changes in the heat release rate in both n-heptane and ethanol dominant mixtures are associated with the concentration change of certain species in the high-temperature zone.

In n-heptane-dominant mixtures, the investigation reveals that steady-state species at the high-temperature zone, including hydroxyl radicals (OH) and hydroperoxyl radicals (HO₂), maintain the equilibrium between production and consumption rate, directly affecting heat release rate. Non-steady-state species at the high-temperature zone, such as CH₂O and C₂H₄ play significant roles in the auto-ignition process, primarily due to their involvement in LTC at the low-temperature zone and subsequent species diffusion to the high-temperature region.

For ethanol-dominant mixtures, the study highlights the observed increase in heat release rate with the increase in ethanol's volume fraction, attributing this elevation to the decomposition of ethanol into major products including CH₃CHOH, CH₂CH₂OH and CH₃CH₂O radicals. The production of these species, particularly through hydrogen abstraction reactions, is identified as the key pathway driving the observed increase in heat release rate.

Using the proposed method, we identified the key species involved in diffusion and demonstrate how the diffusion of these species bridges the low and high temperature zones in n-heptane-dominant mixtures. Additionally, the analysis results indicates, in the ethanol dominant mixtures, chemical kinetics are notably unaffected by n-heptane's LTC, highlighting the distinctive chemical pathways of ethanol and the influence of fuel composition on heat release rate and auto-ignition.

4. Conclusion and outlook

This work proposed a method of analysis to reveal the relationship between change in heat release rate and variations of species, elucidating interaction among related species and the potential influence of species transport across different temperature zones in reactive field.

For demonstration, the study investigated the auto-ignition temperature of n-heptane and ethanol mixtures in a counterflow flame configuration under low strain rates. The analysis results indicate that this method effectively quantifies and compares the influence of chemical kinetics and species diffusion effects, detailing the complex interactions of critical species that influence the heat release rate.

Future research directions may include applying the method of analysis under varying strain rates and extending to other one-dimensional flame configurations. Additionally, given the complexity of preparing the overview for various mixtures, future efforts will focus on streamlining the analysis process through enhancing code automation.

Appendix A. Concentration Analysis Results

Appendix A.1. *n*-Heptane Dominant Mixtures

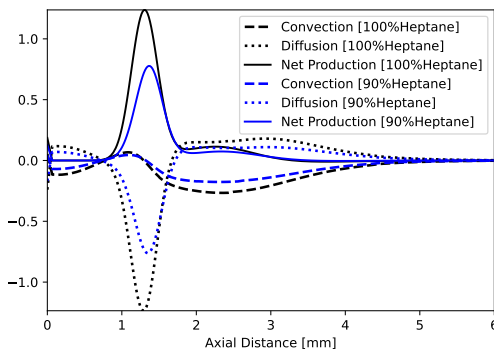


Figure A.20: C_2H_4 Species equation terms

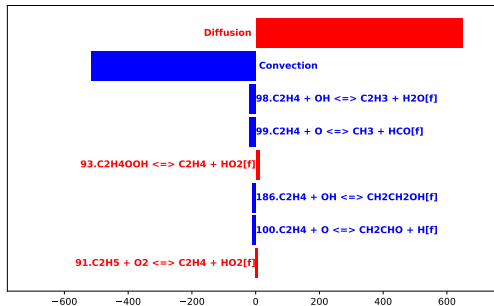


Figure A.21: Contribution on C_2H_4 concentration change @4.2mm

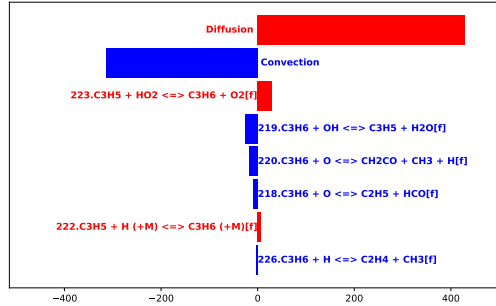


Figure A.22: Contribution on C_3H_6 concentration change @4.2mm

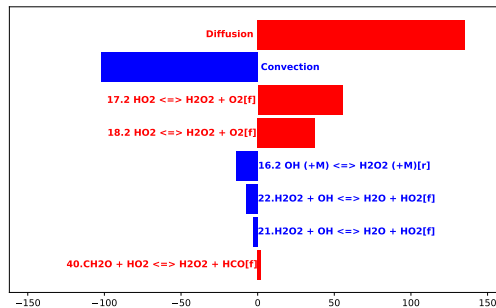


Figure A.23: Contribution on H_2O_2 concentration change @4.2mm

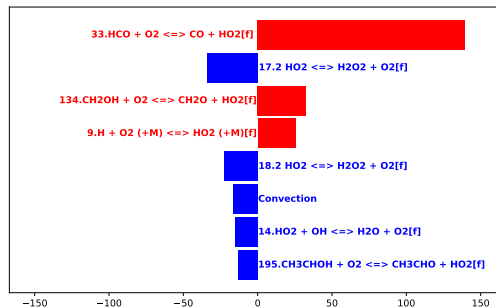


Figure A.24: Contribution on HO_2 concentration change @4.2mm

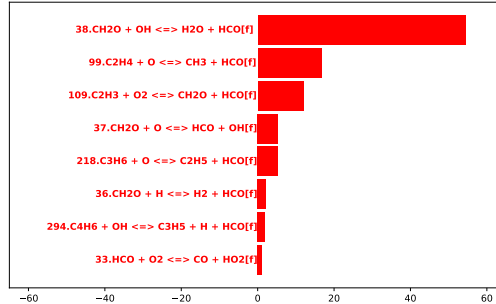


Figure A.25: Contribution on HCO concentration change @4.2mm

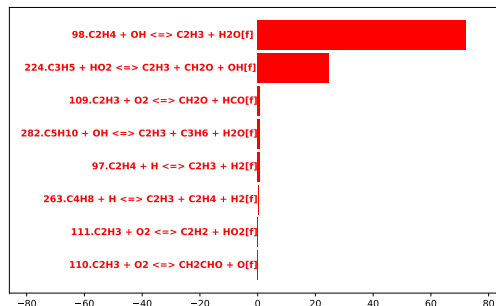


Figure A.26: Contribution on C₂H₃ concentration change @4.2mm

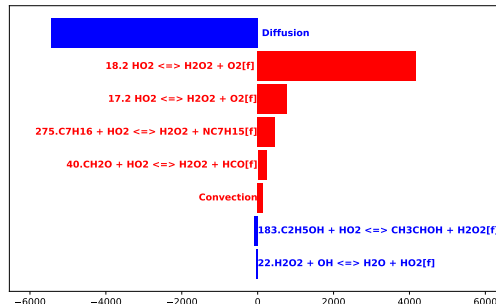


Figure A.27: Contribution on H₂O₂ concentration change @1.1mm

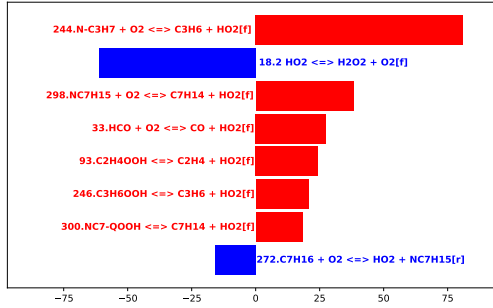


Figure A.28: Contribution on HO₂ concentration change @1.1mm

Appendix A.2. Ethanol Dominant Mixtures

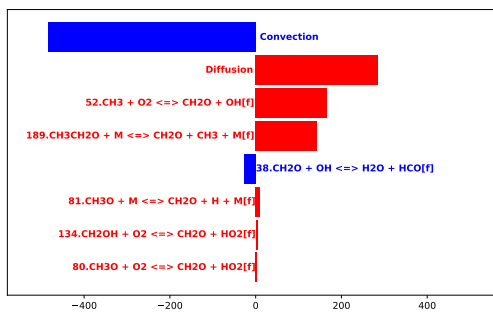


Figure A.29: Contribution on CH₂O concentration change @4.2mm

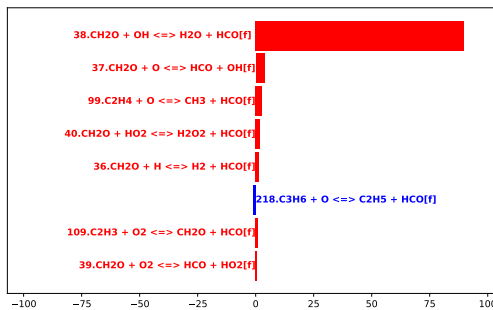


Figure A.30: Contribution on HCO concentration change @4.2mm

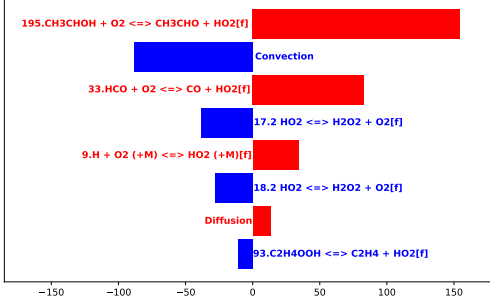


Figure A.31: Contribution on HO₂ concentration change @4.2mm

Appendix B. Details of Derivation of Analysis Method

Appendix B.1. Derivation of reaction-rate-change-analysis

The first-order derivatives, $\partial\dot{\omega}_n/\partial k_n$ and $\partial\dot{\omega}_n/\partial c_i$, correspond to the changes caused by variations in individual variables. However, the reaction rate expression, $\dot{\omega}_n$, is a multivariate function. For instance, $\dot{\omega}_{f,k} = k_{f,k} \prod_{i=1}^m c_i^{\nu'_i}$ and $\dot{\omega}_{b,k} = k_{b,k} \prod_{i=1}^m c_i^{\nu''_i}$. Therefore, to enhance precision, it is essential to consider the reaction rate changes resulting from the mutual influence of variables. For this purpose, the second-order Taylor expansion can be employed, offering a more comprehensive understanding and accurate calculation.

The formula below outlines the approximated reaction rate from the second-order Taylor expansion for function of multiple variables:

$$\Delta\dot{\omega}_n^{\text{approx}} = \sum_{i=0}^m \frac{\partial\dot{\omega}_n}{\partial x_i} \Delta x_i + \frac{1}{2} \sum_{i=0}^m \sum_{j=0}^m \frac{\partial^2\dot{\omega}_n}{\partial x_i \partial x_j} \Delta x_i \Delta x_j \quad (\text{B.1})$$

For simplification, let the variable x_i encompasses both the rate constant, k_n , and the species concentration, c_i , with x_0 specifically denoting k_n .

$$x_i = \begin{cases} k_n, i = 0 \\ c_i, i \neq 0 \end{cases} \quad \text{where } i = 0, 1, \dots \quad (\text{B.2})$$

By employing the second derivative in Taylor series, the change in reaction rate attributed to Δx_i could be written as:

$$\Delta\dot{\omega}_n|_{x_i} = \frac{\partial\dot{\omega}_n}{\partial x_i} \Delta x_i + \frac{1}{2} \frac{\partial^2\dot{\omega}_n}{\partial x_i^2} (\Delta x_i)^2 + \sum_{\substack{j=0 \\ j \neq i}}^m \frac{1}{2} \frac{\partial^2\dot{\omega}_n}{\partial x_i \partial x_j} \Delta x_i \Delta x_j \quad (\text{B.3})$$

The term $\frac{\partial \dot{\omega}_n}{\partial x_i} \Delta x_i + \frac{1}{2} \frac{\partial^2 \dot{\omega}_n}{\partial x_i^2} (\Delta x_i)^2$ delineates the direct contribution of Δx_i to $\Delta \dot{\omega}_n$, encapsulating both linear and quadratic influences. While, the term $\frac{1}{2} \frac{\partial^2 \dot{\omega}_n}{\partial x_i \partial x_j} \Delta x_i \Delta x_j$ quantifies the synergistic influence on $\Delta \dot{\omega}_n$ emanating from interaction between Δx_i and Δx_j . This synergistic influence could be symmetrically attributed to the influence from both Δx_i and Δx_j .

Appendix B.2. Derivation of species concentration change

For the counterflow flame, in steady state solution, governing equation for species i is given by :

$$0 = -\rho u \frac{dY_i}{dz} - \frac{dj_i}{dz} + W_i (\dot{\omega}_i^+ - \dot{\omega}_i^-) \quad (\text{B.4})$$

Here, W_i denotes the molecular weight of species i . The production rate of species i is represented by $\dot{\omega}_i^+$, while $\dot{\omega}_i^-$ symbolizes the consumption rate of species i . The production and consumption rate can be expressed as follows:

$$\begin{aligned} \dot{\omega}_i^+ &= \sum_{k=1}^r \nu_{i,k} [(1 - \delta'_{i,k}) \dot{\omega}_{f,k} - \delta'_{i,k} \dot{\omega}_{b,k}] \\ &= \sum_{k=1}^r |\nu_{i,k}| [(1 - \delta'_{i,k}) \dot{\omega}_{f,k} + \delta'_{i,k} \dot{\omega}_{b,k}] \end{aligned} \quad (\text{B.5})$$

$$\begin{aligned} \dot{\omega}_i^- &= \sum_{k=1}^r \nu_{i,k} [-\delta'_{i,k} \dot{\omega}_{f,k} + (1 - \delta'_{i,k}) \dot{\omega}_{b,k}] \\ &= \sum_{k=1}^r |\nu_{i,k}| [\delta'_{i,k} \dot{\omega}_{f,k} + (1 - \delta'_{i,k}) \dot{\omega}_{b,k}] \end{aligned} \quad (\text{B.6})$$

with $\delta'_{i,k}$ defined as

$$\delta'_{i,k} = \begin{cases} 1 & \text{if } \nu_{i,k} < 0, \\ 0 & \text{if } \nu_{i,k} > 0 \end{cases} \quad (\text{B.7})$$

The term

$$\nu_{i,k} = \nu''_{i,k} - \nu'_{i,k}$$

where $\nu'_{i,k}$, $\nu''_{i,k}$ are the stoichiometric coefficients for species i appearing as a reactant and as a product in k^{th} reaction, respectively.

Governing equation of species i , Eqn.(B.4), could be rewritten as :

$$\dot{\omega}_i^- = -\rho u \frac{dY_i}{dz}/W_i - \frac{d\dot{j}_i}{dz}/W_i + \dot{\omega}_i^+ \quad (\text{B.8})$$

While, $\dot{\omega}_i^-$ can be expressed as:

$$\dot{\omega}_i^- = c_i \times \sum_{k=1}^r |\nu_{i,k}| [\delta'_{i,k} w_{f,k}^{den} + (1 - \delta'_{i,k}) w_{b,k}^{den}] \quad (\text{B.9})$$

where $w_{f,k}^{den}$, $w_{b,k}^{den}$ are defined as:

$$w_{f,k}^{den} = k_{f,k} \prod_{j=1}^n c_i^{\nu'_j - \delta_{i,j}}, w_{b,k}^{den} = k_{b,k} \prod_{j=1}^n c_i^{\nu''_j - \delta_{i,j}} \quad (\text{B.10})$$

and $\delta_{i,j}$ indicates whether species j is species i :

$$\delta_{i,j} = \begin{cases} 1 & \text{if the species } j \text{ is species } i, \\ 0 & \text{otherwise.} \end{cases} \quad (\text{B.11})$$

Combining the Eqn. (B.8) and Eqn. (B.9), the concentration of substance i , c_i can be derived from following expression:

$$c_i = \frac{-\rho u \frac{dY_i}{dz}/W_i - \frac{d\dot{j}_i}{dz}/W_i + \dot{\omega}_i^+}{\sum_{k=1}^r |\nu_{i,k}| [\delta'_{i,k} w_{f,k}^{den} + (1 - \delta'_{i,k}) w_{b,k}^{den}]} \quad (\text{B.12})$$

Upon substituting Eqn. (B.5) into the equation above, we could obtain a detailed expression for c_i as:

$$c_i = \frac{-\rho u \frac{dY_i}{dz}/W_i - \frac{d\dot{j}_i}{dz}/W_i + \sum_{k=1}^r |\nu_{i,k}| [(1 - \delta'_{i,k}) \dot{\omega}_{f,k} + \delta'_{i,k} \dot{\omega}_{b,k}]}{\sum_{k=1}^r |\nu_{i,k}| [\delta'_{i,k} w_{f,k}^{den} + (1 - \delta'_{i,k}) w_{b,k}^{den}]} \quad (\text{B.13})$$

References

- [1] H. Tsuji, Counterflow diffusion flames, *Progress in Energy and Combustion Science* 8 (1982) 93–119. URL: <https://www.sciencedirect.com/science/article/pii/0360128582900156>. doi:[https://doi.org/10.1016/0360-1285\(82\)90015-6](https://doi.org/10.1016/0360-1285(82)90015-6).
- [2] K. Seshadri, F. A. Williams, Laminar flow between parallel plates with injection of a reactant at high reynolds number, *International Journal of Heat and Mass Transfer* 21 (1978) 251–253. doi:[https://doi.org/10.1016/0017-9310\(78\)90230-2](https://doi.org/10.1016/0017-9310(78)90230-2).
- [3] R. Seiser, H. Pitsch, K. Seshadri, W. Pitz, H. Gurran, Extinction and autoignition of n-heptane in counterflow configuration, *Proceedings of the Combustion Institute* 28 (2000) 2029–2037. doi:[https://doi.org/10.1016/S0082-0784\(00\)80610-4](https://doi.org/10.1016/S0082-0784(00)80610-4).
- [4] L. Ji, A. Cuoci, A. Frassoldati, M. Mehl, T. Avedisian, K. Seshadri, Experimental and computational investigation of the influence of iso-butanol on autoignition of n-decane and n-heptane in non-premixed flows, *Proceedings of the Combustion Institute* 39 (2023) 2007–2015. doi:<https://doi.org/10.1016/j.proci.2022.08.058>.
- [5] H. Rabitz, M. Kramer, D. Dacol, Sensitivity analysis in chemical kinetics, *Annual Review of Physical Chemistry* 34 (1983) 419–461. URL: <https://api.semanticscholar.org/CorpusID:97123635>.
- [6] T. Turanyi, Applications of sensitivity analysis to combustion chemistry, *Reliability Engineering and System Safety* 57 (1997) 41–48. doi:[https://doi.org/10.1016/S0951-8320\(97\)00016-1](https://doi.org/10.1016/S0951-8320(97)00016-1), the Role of Sensitivity Analysis in the Corroboration of Models and its Links to Model Structural and Parametric Uncertainty.
- [7] T. A. O. Kalen Braman, V. Raman, Adjoint-based sensitivity analysis of flames, *Combustion Theory and Modelling* 19 (2015) 29–56. doi:[10.1080/13647830.2014.976274](https://doi.org/10.1080/13647830.2014.976274).
- [8] W. Sun, Z. Chen, X. Gou, Y. Ju, A path flux analysis method for the reduction of detailed chemical kinetic mechanisms, *Combustion and Flame* 157 (2010) 1298–1307. doi:<https://doi.org/10.1016/j.combustflame.2010.03.006>.
- [9] W. Wang, X. Gou, An improved path flux analysis with multi generations method for mechanism reduction, *Combustion Theory and Modelling* 20 (2016) 203–220. doi:[10.1080/13647830.2015.1117660](https://doi.org/10.1080/13647830.2015.1117660).
- [10] W. Ji, W. Qiu, Z. Shi, S. Pan, S. Deng, Stiff-pinn: Physics-informed neural network for stiff chemical kinetics, *The Journal of Physical Chemistry A* 125 (2021) 8098–8106.
- [11] Y. Weng, D. Zhou, Multiscale physics-informed neural networks for stiff chemical kinetics, *The Journal of Physical Chemistry A* 126 (2022) 8534–8543. URL: <https://doi.org/10.1021/acs.jpca.2c06513>. doi:[10.1021/acs.jpca.2c06513](https://doi.org/10.1021/acs.jpca.2c06513), pMID: 36322833.
- [12] X. Su, W. Ji, J. An, Z. Ren, S. Deng, C. K. Law, Kinetics parameter optimization of hydrocarbon fuels via neural ordinary differential equations, *Combustion and Flame* 251 (2023) 112732. URL: <https://www.sciencedirect.com/science/article/pii/S0010218023001177>. doi:<https://doi.org/10.1016/j.combustflame.2023.112732>.
- [13] J. M. Zurada, A. Malinowski, S. Usui, Perturbation method for deleting redundant inputs of perceptron networks, *Neurocomputing* 14 (1997) 177–193. doi:[https://doi.org/10.1016/S0925-2312\(96\)00031-8](https://doi.org/10.1016/S0925-2312(96)00031-8).

- [14] F. Williams, Combustion Theory. 2nd edition, 1985. URL: <https://www.osti.gov/biblio/5936474>. doi:<https://doi.org/10.1201/9780429494055>.
- [15] S. Liu, J. C. Hewson, J. H. Chen, H. Pitsch, Effects of strain rate on high-pressure non-premixed n-heptane autoignition in counterflow, Combustion and Flame 137 (2004) 320–339. doi:<https://doi.org/10.1016/j.combustflame.2004.01.011>.
- [16] J. Herzler, L. Jerig, P. Roth, Shock tube study of the ignition of lean n-heptane/air mixtures at intermediate temperatures and high pressures, Proceedings of the Combustion Institute 30 (2005) 1147–1153. doi:<https://doi.org/10.1016/j.proci.2004.07.008>.
- [17] C. Xie, M. Lailliau, G. Issayev, Q. Xu, W. Chen, P. Dagaut, A. Farooq, S. M. Sarathy, L. Wei, Z. Wang, Revisiting low temperature oxidation chemistry of n-heptane, Combustion and Flame 242 (2022) 112177. doi:<https://doi.org/10.1016/j.combustflame.2022.112177>.
- [18] T. I. Farouk, F. L. Dryer, Isolated n-heptane droplet combustion in microgravity: “cool flames” – two-stage combustion, Combustion and Flame 161 (2014) 565–581. doi:<https://doi.org/10.1016/j.combustflame.2013.09.011>.
- [19] J. Zhang, S. Niu, Y. Zhang, C. Tang, X. Jiang, E. Hu, Z. Huang, Experimental and modeling study of the auto-ignition of n-heptane/n-butanol mixtures, Combustion and Flame 160 (2013) 31–39. doi:<https://doi.org/10.1016/j.combustflame.2012.09.006>.
- [20] S. Guo, A. Cuoci, Y. Wang, C. T. Avedisian, L. Ji, K. Seshadri, N. DiReda, F. Alessio, Combustion Characteristics of a Tier II Gasoline Certification Fuel and its Surrogate with Iso-butanol: experiments and detailed numerical modeling, Technical Report, American Chemical Society, Chicago, Ill., 2022.
- [21] L. Ji, K. Seshadri, F. A. Williams, Experimental and computational investigation of the influence of ethanol on auto-ignition of n-heptane in non-premixed flows, 2024. [arXiv:2406.08507](https://arxiv.org/abs/2406.08507).
- [22] D. G. Goodwin, Moffat, H. K, S. Ingmar, Speth, R. L, Weber, B. W., Cantera: An object-oriented software toolkit for chemical kinetics, thermodynamics, and transport processes., 2023. doi:[10.5281/zenodo.8137090](https://doi.org/10.5281/zenodo.8137090), version 3.0.0.
- [23] The San Diego Mechanism, <http://web.eng.ucsd.edu/mae/groups/combustion/mechanism.html>, 2016.
- [24] S. M. Sarathy, P. Oßwald, N. Hansen, K. Kohse-Höinghaus, Alcohol combustion chemistry, Progress in Energy and Combustion Science 44 (2014) 40–102. URL: <https://www.sciencedirect.com/science/article/pii/S0360128514000240>. doi:<https://doi.org/10.1016/j.pecs.2014.04.003>.